Identification of a Guanine Binding Domain Peptide of the GTP Binding Site of Glutamate Dehydrogenase: Isolation with Metal–Chelate Affinity Chromatography†

Michael T. Shoemaker and Boyd E. Haley*

Division of Medicinal Chemistry & Pharmaceutics, College of Pharmacy and the Markey Cancer Center, University of Kentucky Medical Center, 800 Rose Street, Lexington, Kentucky 40536-0093

Received September 9, 1992; Revised Manuscript Received December 11, 1992

ABSTRACT: Photoaffinity labeling with [α-^{32}P]8N_3GTP and [γ-^{32}P]8N_3GTP was used to identify the guanine binding domain of the GTP regulatory site within glutamate dehydrogenase (GDH). Without photolysis, 8N_3GTP mimicked the regulatory properties of GTP on GDH activity with 8N_3GTP exhibiting a K_i of 5 μM while the K_i for GTP was about 0.6 μM. Under optimal photolabeling conditions saturation of photoinsertion with 1 μg of GDH revealed an apparent K_d of 9 ± 4 μM for [γ-^{32}P]8N_3GTP. Photolabeling with this analog could be competitively inhibited with GTP with an apparent K_d of 12 ± 2 μM. Other nucleotides such as ATP and NAD(P)H could not reduce the amount of photoinsertion as effectively as GTP. ADP could decrease photoinsertion, but only at much higher concentrations. NAD(P)$^+$, GDP, AMP, and GMP had little effect on photoinsertion. Divalent cations Mg^{2+} and Ca^{2+} also reduced photoinsertion significantly while the monovalent K^+ and Na^+ ions had no effect. Aluminum(III)–chelate or iron(III)–chelate affinity chromatography and reversed-phase HPLC were used to purify photolabel-containing peptides generated with either trypsin or chymotrypsin. This identified a portion of the guanine binding domain within the GTP regulatory site as the region containing the sequence Ile439 to Tyr454. Photolabeling of this peptide was prevented 91% by the presence of 300 μM GTP during photolysis. Lys445 was not identified in sequence analyses of the photolabeled peptides. Also, trypsin was unable to cleave the photolabeled peptide at this site. These results suggest that Lys445 may be the residue modified by [α-^{32}P]8N_3GTP.

Mammalian glutamate dehydrogenase (GDH, EC 1.4.1.3) is involved with integration of amino acid metabolism via the tricarboxylate cycle. This enzyme also has a significant role in controlling the levels of ammonia and glutamate, a ubiquitous neurotransmitter within the central nervous system (Fonnum, 1984). Bovine liver GDH catalyzes the forward and reverse reaction of oxidatively deaminating 1-glutamate into α-ketoglutarate and NH_4^+. The enzyme is able to use NADH or NADPH with comparable efficacy as an electron source for the reverse reaction. It has been implicated in the etiology of a variety of diseases including olivopontocerebellar degeneration (OPCA) and Parkinson's and Reye's syndrome (Plaitakis & Berl, 1988; Tipton & Couee, 1988).

Bovine liver GDH is composed of six identical subunits (56 kDa/subunit) of which the primary sequence has been published (Moon et al., 1972). The regulation of glutamate dehydrogenase is very complex. It has been shown that leucine and other factors regulate the activity of this enzyme (Erecinska & Nelson, 1990; Fahien et al., 1990). However, the main regulators of this enzyme are nucleotides. One nucleotide regulator, NAD^+, is also a substrate for the forward enzymatic reaction by providing the oxidating potential. Utilizing the photoprobe [α-^{32}P]2$N_3$$NAD^+$,[1] which is also a substrate for GDH, the adenine binding domain within the NAD^+ binding site was isolated and identified (Kim & Haley, 1991). This isolation used boronate chromatography, which took advantage of extended cis-diol of the nicotinic ribose sugar to selectively bind the photolabeled peptide.

Each subunit also contains both an ADP and GTP regulatory site(s) which activates and inhibits enzyme activity, respectively. The 8-azidopurine analogs of ADP and GTP have also been tested, and they mimic the regulatory activities of these native nucleotides. However, peptides photolabeled with the photoprobes of ADP and GTP were not tractable to isolation by boronate chromatography. This is probably due to the close proximity of the single cis-diol to the peptide and the charge repulsion between the polyphosphate and the immobilized boronate anion.

Identifying nucleotide binding sites has been advanced by the use of nucleotide photoaffinity analogs which selectively insert into a site upon photoactivation with ultraviolet light (King et al., 1991). Using an analog of GTP, 8N_3GTP, the GTP binding site of glucagon was isolated and identified (Shoemaker et al., 1992). A major improvement in isolating nucleotide binding sites modified by various azidonucleotide photoprobes is the use of metal–chelate affinity resins. These resins were first used to bind molecules and proteins that were phosphorylated (Anderson, 1991; Scanff et al., 1991). They are also excellent for isolating the peptides covalently modified with azidonucleotides through coordination of the iminodiacetate-chelated metal ion with the photoinserted phosphate moiety. Recently, this laboratory has used Fe–chelate affinity chromatography to identify the ATP and AMP binding sites within chicken muscle adenylate kinase (Salvucci et al., 1992) as well as the nucleotide binding sites within rmGM-CSF (Doukas et al., 1992) and Botulinum toxin C3 enzyme (Chavan et al., 1992).

† This work was supported by National Institutes of Health Research Grant GM-35766 and the Lexington Clinic Foundation.

* Corresponding author.

[1] Abbreviations: 2$N_3$$NAD^+$, 2-azidonicotinamide adenine dinucleotide; 8N_3GTP, 8-azidoguanosine 5′-triphosphate; SDS–PAGE, sodium dodecyl sulfate–polyacrylamide gel electrophoresis; 8N_3ADP, 8-azidoadenosine 5′-diphosphate; PTH, phenylthiohydantoin.

0006-2960/93/0432-1883$04.00/0

In the present study, [γ-^{32}P]8N_3GTP and [α-^{32}P]8N_3GTP were used to specifically photoaffinity label bovine liver GDH. Aluminum(III)–chelate chromatography and iron(III)–chelate affinity chromatography were used in conjunction with reversed-phase HPLC to isolate the peptide sequence within GDH that is specifically photolabeled by [α-^{32}-P]8N_3GTP. Al^{3+}–chelate affinity chromatography has been used to identify the azidonucleotide-modified peptides in β-tubulin.[2] In this paper, aluminum(III)–chelate chromatography is shown to be an effective technique for isolating and identifying peptides modified with photoaffinity nucleotide probes.

MATERIALS AND METHODS

[γ-^{32}P]8N_3GTP and [α-^{32}P]8N_3GTP (9–20 mCi/μmol) were prepared and purified as previously reported (Geahlen & Haley, 1977; Potter & Haley, 1983). Molecular weight standards were obtained from Bio-Rad. Bovine glutamate dehydrogenase (GDH), trypsin, and chymotrypsin and all other reagents were obtained from Sigma Chemical Co. and were analytical grade.

Enzymatic Assay. The activity of purified GDH was determined by measuring the reduction rate of NAD^+ at 23 °C. GDH (16.6 μg) was incubated with 40 mM glutamate, 50 μm EDTA, and 400 μM NAD^+ in 20 mM Tris–HOAc buffer, pH 8.0 (total volume 1 mL), in the presence or absence of effector molecules. The initial appearance rate of NADH was determined by measuring the optical density of the solution at 340 nm on a Beckman DU-70 spectrophotometer. The measurements were taken from 0 to 2 min after the addition of GDH.

Photolabeling of Glutamate Dehydrogenase. For saturation studies, 1 μg of glutamate dehydrogenase in 5 mM Tris–acetate buffer, pH 7.1, was incubated with the appropriate concentration of the photoprobe [γ-^{32}P]8N_3GTP or [α-^{32}P]-8N_3GTP in Eppendorf tubes for 20 s. The sample was then irradiated with a handheld 254-nm Mineralight UVS-11 UV lamp (I = 4600 μW/cm^2) for 75 s from a distance of 1 cm at 4 °C. The total reaction volume was 40 μL. The reaction was quenched by the addition of 40 μL of cold 7% trichloroacetic acid (TCA). The reaction mixture was kept at 4 °C for 15 min and then centrifuged in a Fisher Scientific microcentrifuge, Model 235C, for 10 min. The supernatant was drawn off and the pellet was resuspended in a protein solubilizing mix (PSM) consisting of 200 mM Tris buffer, 10% SDS, 3.6 M urea, 2.5% (w/v) DTT, and 2% (w/v) pyroinin Y, pH 8.0, in preparation for SDS–PAGE.

For effector and competition studies, 1 μg of GDH was incubated with the competitor for 15 s in buffer at 4 °C prior to the addition of [γ-^{32}P]8N_3GTP and then allowed to incubate with the photoprobe for 1 min. The reaction mixture was irradiated, quenched, and prepared for SDS–PAGE as described above.

SDS–PAGE, Scintillation, and Laser Densitometry. Photolabeled samples were subjected to SDS–PAGE on a 10% acrylamide gel and dried on a slab gel dryer. Autoradiography of the dried gels was usually complete after 4–8 h. ^{32}P incorporation into protein bands was determined by excision of the gels followed by scintillation counting in a Packard Minaxi Tri-Carb liquid scintillation system, Model B4430 (99% efficient). The bands from the autoradiogram were scanned on an image aquisition densitometer (BioImage; MilliGen/Bioresearch, Ann Arbor, MI).

[2] B. Jayaram and B. Haley, manuscript in preparation.

Photolabeling and Enzymatic Digestion of GDH. To determine the site modified by [α-^{32}P]8N_3GTP, 1 mg of GDH in 5 mM Tris–acetate buffer (pH 8.0) was incubated with 50 μM [γ^{32}P]8N_3GTP or [α-^{32}P]8N_3GTP (total volume 1.85 mL) for 90 s at 4 °C in disposable beakers from Fisher Scientific. Some experiments were performed in 5 mM K_2HPO_4 buffer (pH 8.0). The mixture was irradiated for 75 s. For the second photolysis, nonradioactive 8N_3GTP was then added (to a final concentration 50 μM) and incubated for 90 s, and the reaction mixture was again irradiated for 90 s. The reaction was quenched by the addition of 2.45 mL of cold TCA (7%), transferred to a 15-mL Corex test tube, and kept at 4 °C for 15 min. The protein was precipitated by centrifugation at 2000 rpm for 15 min in a Beckman Model TJ-6 centrifuge at 0 °C. The supernatant was drawn off, and the pellet was resuspended in 667 μL of solution containing a final concentration of 2 M urea in 75 mM NH_4HCO_3; the pH was adjusted to 8.5–9.0 by the addition of 5 M NH_4OH.

GDH was proteolyzed by the addition of 7.5 μg of chymotrypsin or trypsin and kept at room temperature for 3 h after which 7.5 μg of the respective protease was added again. After 3 more hours at room temperature, 10 μg of the same protease was added, and the digestion mix was kept at 25 °C overnight.

To validate that the isolated peptide(s) was specific for the GTP site and could be protected from photomodification, the sample was photolyzed in the presence of 300 μM GTP and proteolyzed as described above.

Ion-Exclusion Chromatography. Separation of the photolabeled peptides from the bulk of nonacidic peptides was accomplished using a sulfopropyl-Sephadex C25 (SP 25) resin. Sodium formate buffer, pH 3.5, was added to the digested samples (3:1), and the pH was adjusted to 3.5–4.0 by the addition of formic acid. The samples were loaded onto a column (30 × 1.5 cm) equilibrated in the same buffer. The eluate was monitored for radioactivity to determine the location of the radiolabeled peptide, and these fractions were collected and prepared for metal–chelate affinity chromatography.

Immobilized Metal–Chelate Affinity Chromatography. Preparation of the iron(III)–chelate column was as follows: 400 μL of resin, iminodiacetic acid–epoxy-activated Sepharose 6B fast flow, amberlite, or polystyrene supports (Sigma) were washed and chelated with Fe^{3+} by slowly (0.25 mL/min) passing through a 50 mM $FeCl_3$ solution after which the resin was washed wth 10 mL of H_2O and then 10 mL of 100 mM NH_4OAc, pH 8.0 (buffer A). The column was then washed with 5 mL each of 4 M urea in buffer A (buffer B) and then buffer A. Washes of 0.5 M NaCl in buffer A (buffer C) and buffer A, respectively, were then applied to the column. Preparation of the sample was as follows: buffer A was added to the radioactive flow-through from SP 25 chromatography; the pH of this sample was adjusted to 8–8.5, and the sample was loaded onto the metal–chelate column (0.5 mL/min) at 25 °C. Ten milliliters of buffer A was passed through the column. The column was then washed with 10 mL each of buffer B, buffer A, buffer C, and buffer A, respectively. The modified peptides were eluted from the resin by passing through 5 mM K_2HPO_4 in buffer A (buffer D). One-milliliter fractions were collected, and radioactivity was determined by liquid scintillation counting.

For preparation of the aluminum(III)–chelate column, 1.4 mL of the resin was washed and chelated with Al^{3+} by slowly passing through 20 mL of 50 mM $AlCl_3$. The resin was then washed with H_2O, 50 mM NH_4OAc, pH 5.8 (buffer E), and 0.5 M NaCl in buffer E (buffer F). Buffer E was added to

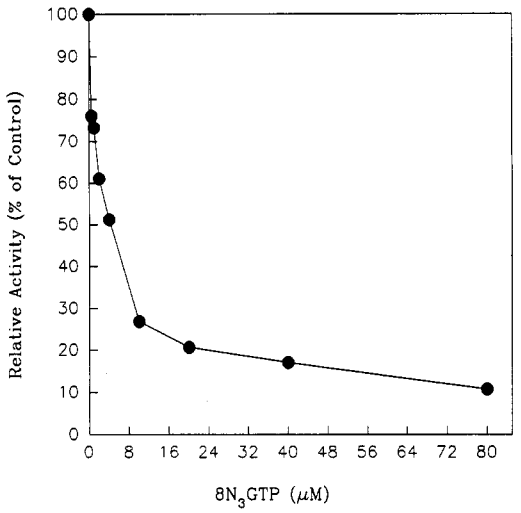

FIGURE 1: Effect of $8N_3GTP$ on GDH activity. The activity of GDH was measured as described in Materials and Methods. The incubation mixture was preincubated with increasing concentrations of $8N_3GTP$. The activity was measured as the increase in absorbance at 340 nm after 20 s.

the digestion mixture (1:1). The pH was adjusted to 5.8 with acetic acid, and the sample was loaded onto the column. The column was washed with approximately 15 mL of buffer E and 10 mL of buffer F. The radiolabeled peptides were eluted with 5 mL of buffer D.

HPLC and Sequencing of Photolabeled Peptides. The digestion mix was subjected to SP 25 and Fe^{3+} or Al^{3+} chromatography as described, and the radioactive fractions were concentrated in a Savant speedvac concentrator until the volume was below 1.5 mL. The samples were then subjected to reversed-phase HPLC using an aquapore RP 300 C_8 column (Brownlee Lab) on a LKB HPLC system equipped with a diode array spectral detector. The mobile system consisted of a 25 μM $AlCl_3$/0.1% TFA solution (X) and 0.1% TFA/70% acetonitrile (Y) solvent system. The gradient for HPLC was 0–10 min, 0% Y; and 10–70 min, 0–100% Y at a flow rate 0.5 mL/min. HPLC fractions containing photolabeled peptides were sequenced on an Applied Biosystem 477A protein sequencer with an on-line PTH[1] identification.

RESULTS

To show that $8N_3GTP$ could mimic the regulatory properties of GTP, the photoanalog should be able to reversibly inhibit GDH in the absence of activating light. This probe has previously been shown to mimic GTP in supporting tubulin polymerization and activating adenylyl cyclase (Geahlen & Haley, 1979; Hoyer et al., 1986). In enzymatic assays $8N_3$-GTP was able to inhibit GDH with a K_i of 5 μM (Figure 1). A similar K_i has been reported for GTP (McCarthy & Tipton, 1984; Frieden, 1963). However, in this study GTP was able to inhibit GDH activity more effectively (K_i = 0.6 μM). Maximal inhibition of GDH occurred with either 60 μM GTP or 100 μM $8N_3GTP$ and was 95% which is the same as others have reported (Pal & Colman, 1979). Similarly, $8N_3ADP$ was able to increase the activity of GDH to the same degree as ADP (data not shown). These results show that the azidonucleotides are able to elicit nearly the same biological effect upon GDH as the natural nucleotides.

To show the specificity of the [α-^{32}P]$8N_3GTP$–GDH interaction, photoinsertion of the azidonucleotide should exhibit activating UV light dependency and saturation effects.

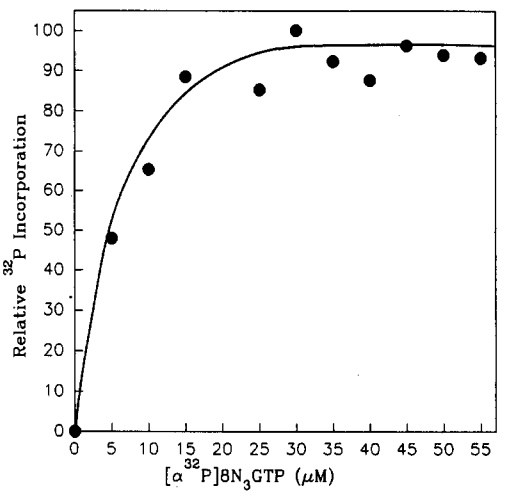

FIGURE 2: Saturation of [α-^{32}P]$8N_3GTP$ photoinsertion into glutamate dehydrogenase. One microgram of GDH in 40 μL of reaction buffer was photolyzed with the indicated concentration of [α-^{32}P]$8N_3GTP$ and subjected to SDS–PAGE. ^{32}P incorporation was detected by autoradiography and quantified by laser densitometry. One hundred percent photoincorporation corresponds to 251 integrated OD units from the autoradiogram as determined by laser densitometry. Photoincorporation was quantitatively confirmed by cutting the appropriate band and determining radioactivity by liquid scintillation counting.

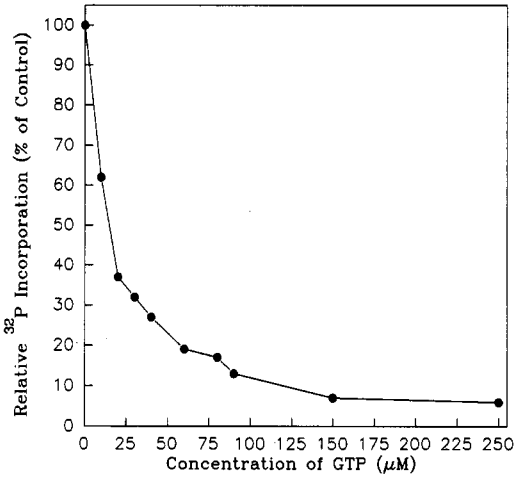

FIGURE 3: Prevention of [α-^{32}P]$8N_3GTP$ photoinsertion into GDH by GTP. Forty micromolar [α-^{32}P]$8N_3GTP$ was incubated with 1 μg of GDH in the presence of the indicated concentrations of GTP, and the reaction mixture was photolyzed. ^{32}P incorporation was detected by autoradiography and quantified by liquid scintillation.

Also, increasing GTP concentrations should decrease photoinsertion of the probe. When the sample was not irradiated, no labeling was observed. This indicates absence of any phosphorylation under these conditions. When the probe was preirradiated, no covalent modification was observed when GDH was subsequently added. This indicates the absence of any light-generated long-lived chemical intermediates, remaining after irradiation, that could cause pseudophotoaffinity labeling (data not shown). Under the experimental conditions described, photoinsertion of GDH was saturated with [γ-^{32}P]$8N_3GTP$ at about 25–30 μM photoprobe. The apparent K_d of this interaction was 9 ± 4 μM (Figure 2).

The results in Figure 3 show that GTP was able to protect photolabeling from 40 μM [^{32}P]$8N_3GTP$ with an apparent K_d of 12 ± 2 μM. Over 94% protection was observed with 250 μM GTP. GTP has been reported to inhibit GDH with a K_i of 9.5 μM (McCarthy & Tipton, 1984) and 10 μM (Frieden, 1963) in good agreement with this result. Other

Table I: Effect of Various Nucleotides on Photolabeling GDH with 40 μM [γ-^{32}P]8N$_3$GTP

	% of control		
nucleotide	40 μM	150 μM	300 μM
none (100%)			
GTP	23	11	6
GDP	70	50	24
GMP	71	62	71
ATP	42	17	12
ADP	60	44	23
AMP	71	69	66
	% of control		
nucleotide	100 μM	250 μM	500 μM
NAD$^+$	100	50	41
NADH	25	14	8
NADP$^+$	100	94	45
NADPH	24	9	6

nucleotides were able to inhibit photoinsertion, although not as effectively as GTP. GDP and GMP were not as good as inhibitors of photoinsertion as GTP, although 300 μM GDP reduced photoinsertion nearly 76%. ATP inhibited photoinsertion, but not as effectively as GTP. At 300 μM ATP, photoinsertion with [γ-^{32}P]8N$_3$GTP was reduced 88%. ADP was able to reduce photoinsertion, but only at much higher concentrations (Table I).

It has been reported that GDH contains both an NADH-dependent and an NADH-independent GTP binding site (Pal & Colman, 1979). There is some disagreement on whether there are two NADH sites. The data in Figure 2 indicate that under the conditions described only a single K_d is observed. To attempt detection of two different GTP sites, supersaturating concentrations (60 μM) of [γ-^{32}P]8N$_3$GTP were incubated with GDH and increasing amounts of NAD(P)H or NAD(P)$^+$ were added to determine the effect on [γ-^{32}P]8N$_3$-GTP photolabeling of GDH. NAD$^+$ had little effect on photoinsertion. NADH not only did not increase photoinsertion but also reduced photolabeling significantly. NADPH was also able to decrease photolabeling to the same degree as NADH (Table I). Also, saturation studies with [^{32}P]8N$_3$-GTP in the presence of 372 μM NADH were performed. These studies did not reveal a second GTP binding site on GDH even up to concentrations of 250 μM [^{32}P]8N$_3$GTP (data not shown).

The optimal pH for photoinsertion with [γ-^{32}P]8N$_3$GTP or [α-^{32}P]8N$_3$GTP was within the range 6.5–8.5 (data not shown). These studies were conducted using a variety of buffer systems over a pH range of 3.0–9.0. In other studies, metal ions were able to affect labeling of certain proteins with [γ-^{32}P]8N$_3$GTP (Shoemaker et al., 1992; Jayaram and Haley[2]). In the case of GDH, $MgCl_2$ at 1 and 10 mM concentrations reduced photolabeling about 46% and 70%, respectively. It has been previously shown that GTP complexed with Mg^{2+} was unable to inhibit GDH (McCarthy & Tipton, 1984). Our data suggest that this may be due to a decreased affinity of GDH for the Mg–GTP complex. Ca^{2+} was also able to reduce photolabeling although not to the extent of Mg^{2+}. K^+ or Na^+ ions had little effect upon photolabeling GDH with [γ-^{32}P]8N$_3$GTP although at 10 mM, these ions caused a slight increase. EDTA greatly inhibited photolabeling while P_i and PP_i at millimolar concentrations were also able to reduce photolabeling (Table II). Zn^{2+} has been reported to have the same effect as GTP on GDH (Bitensky et al., 1965). This cation had little effect on photolabeling.

Table II: Effect of Ions and Chelators on Photolabeling GDH with [γ-^{32}P]8N$_3$GTP

	% of control		
effector	1 mM	5 mM	10 mM
none (100%)			
$MgCl_2$	54	37	30
$CaCl_2$	51	32	25
KCl	98	112	121
NaCl	98	106	100
K_2HPO_4	47	33	10
EDTA	55	30	17
$Na_4P_2O_7$	37	19	12
$ZnCl_2$	85	79	93
$MnCl_2$	43	34	30

The effect of multiple additions and photolyses of [^{32}P]8N$_3$-GTP on the extent of GDH photolabeling was determined as follows. One hundred micrograms (1.79 nmol of subunit) of GDH was incubated with 50 μM [α-^{32}P]8N$_3$GTP and photolyzed for 75 s. This step was repeated twice. After the second photolabeling, a 50% increase in photoinsertion was observed. However, after the third photolabeling, only a marginal increase in photolabeling was observed. Preirradiation of GDH prior to the addition of photoprobe had no effect on the extent of photolabeling when the photoprobe was subsequently added to the incubation mixture and photolyzed (data not shown).

To identify the peptide sequence within GDH that was modified by 8N$_3$GTP upon photolysis, GDH was photolabeled twice, digested with either trypsin or chymotrypsin, and subjected to multiple chromatography procedures. The enzyme was readily available, so relatively large amounts could be used for peptide mapping. A higher protein to nucleotide ratio is desired to reduce any possible nonspecific labeling. One milligram of GDH in 1.85 mL of reaction mixture was photolabeled when the labeled peptide sequence was determined. This concentration is below the estimated concentration of this enzyme in the mitochondrial matrix (Tomkins et al., 1963), and, reportedly, GDH should be relatively unaggregated at this concentration (Cohen et al., 1976; Tipton & Gouee, 1988).

Photolabeled GDH was separated from most of the noncovalently bound nucleotide by TCA precipitation. After overnight chymotryptic digestion of GDH modified with [α-^{32}P]8N$_3$GTP (see Materials and Methods), the digested sample was added to an anion-exclusion column (SP 25 Sephadex) to remove bulk, nonnegatively charged peptides. The flow-through contained over 95% of the radioactivity (data not shown) which was passed through either an immobilized Fe^{3+}- or an Al^{3+}–chelate affinity column. Earlier reports have shown Fe^{3+}–chelate columns to be able to separate photolabeled peptides from large amounts of nonphotolabeled peptides (Salvucci et al., 1992; Chavan et al., 1992). However, with GDH we obtained better results with the immobilized Al^{3+}–chelate columns (see discussion).

Figure 4 shows the radioactivity profile of the flow-through, wash, and P_i elution fractions for an immobilized Al^{3+}–chelate column which is very similar to that also obtained with the immobilized Fe^{3+}–chelate columns. This is a chymotryptic digest and identical results are obtained regardless of the protease used. Although some radioactivity was found in the flow-through and wash fractions (fractions 1–15), more than 90% of the total radioactivity coeluted with the first four P_i wash fractions (fractions 16–19). The flow-through (fractions 1–5), washes (fractions 6–15), and P_i elution (fractions 16–19) were individually pooled and concentrated in preparation for reversed-phase HPLC.

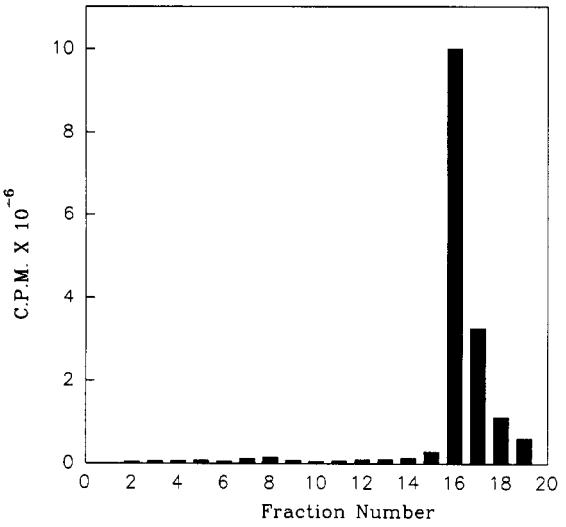

FIGURE 4: Radioactivity profile of chymotryptic peptides eluting from the Al^{3+}–chelate affinity resin. GDH was photolabeled with [α-^{32}P]8N_3GTP, digested with chymotrypsin, and loaded onto an Al^{3+}–chelate affinity column as described in Materials and Methods. Fractions 1–5 and 6–15 represent the fractions collected while loading and washing, respectively. Fractions 16–19 represent fractions eluted with 5 mM K_2HPO_4. Radioactivity was determined by scintillation counting.

The flow-through fractions (1–5) from the immobilized Al^{3+}–chelate column were concentrated and separated by reversed-phase HPLC (Figure 5A). The majority of the peptide fragments were associated with these fractions according to UV absorption analysis from HPLC, especially if the anion-exclusion step was omitted (see Discussion). Also, no major radioactive peaks were observed. The intermediate washes (fractions 6–15) contained no detectable peptide fragments as determined by UV spectrum analysis (data not shown). These data indicate that most of the peptides were not retained on the immobilized Al^{3+} or Fe^{3+} resins. Since most of the peptides are unmodified, they were not expected to bind to the resin. These results were obtained irrespective of the resin support (see Materials and Methods); however, Sepharose 6B fast flow support provided the desired isolation in the shortest equilibration and chromatographic times.

The P_i eluate (fractions 16–19) was subjected to HPLC and the radioactive and OD 210 nm profile is shown in Figure 5B. Three major radioactive peaks were recovered from HPLC. The radioactivity associated with the HPLC flow-through fractions contained no peptides and represents unbound photolyzed or nonphotolyzed [^{32}P]8N_3GTP or probe hydrolyzed from photolabeled peptide during HPLC (King et al., 1991). The two other peaks were collected and concentrated for sequencing. Fractions 35–36 and fraction 41 were collected and sequenced. They were both found to represent the chymotryptic peptide corresponding to residues 436–454. The sequence data are shown in Table III. For both chymotryptic sequences, Lys445 was not identified.

GTP was able to eliminate [α-^{32}P]8N_3GTP photoinsertion into these peptides. GDH was multiply photolyzed as described above in the presence or absence of 300 μM GTP. After digestion with chymotrypsin or trypsin, the digest was subjected to an Al–chelate affinity column and HPLC, respectively. When GTP was originally present in the incubation mixture, the UV and radioactive peaks from HPLC specifically associated with the photolabeled peptides were eliminated (see Figure 5B). This shows that the Al^{3+}–chelate columns effectively retained the photolabeled peptides but did not retain these peptides if they were not photochemically modified.

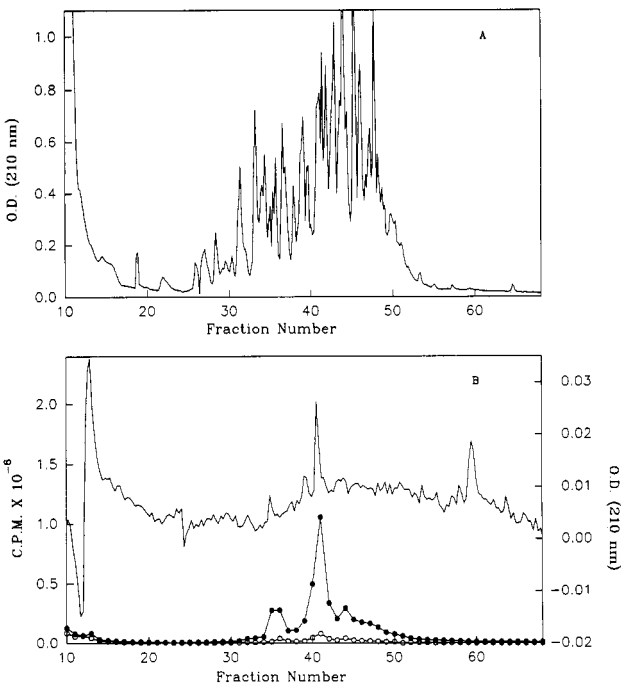

FIGURE 5: Radioactivity profile of HPLC of fractions from Al^{3+}–chelate chromatography. (A) GDH was photolabeled with [α-^{32}P]-8N_3GTP, digested with chymotrypsin and loaded onto an Al^{3+}–chelate affinity column as described in Materials and Methods. The flow-through was loaded onto HPLC. One-minute fractions were collected. The plot represents the OD (210 nm) from the HPLC gradient fractions. Fractions 1–10 represent the HPLC flow-through fractions and were omitted for clarity purposes (see text). (B) The radioactive eluate (fractions 16–19, Figure 4) from Al^{3+}–chelate chromatography was loaded onto HPLC. The plot represents the radioactive profiles from HPLC of the sample photolabeled in the presence (open circles) and absence (closed circles) of GTP (see text). The solid line represents the OD (210 nm) from HPLC of the sample photolabeled in the absence of GTP. ^{32}P incorporation was determined by liquid scintillation.

Table III: Sequence Analyses of Photolabeled Chymotryptic Peptides from the Radioactive Peaks at 35–36 and 41 min in the HPLC Radioactive Profile from Figure 5

		fraction number	
cycle	identified residue	35–36	41
1	Q	*a*	39[b]
2	D	30	36
3	R	26	28
4	I	9	30
5	S	8	16
6	G	18	20
7	A	13	21
8	S	9	8
9	E	7	13
10	K	1	a
11	D	11	9
12	I	4	10
13	V	a	6
14	H	a	3
15	S	a	4
16	G	a	5
17	L	a	5
18	A	a	3
19	Y	a	2

[a] Amino acid not identified. [b] Picomoles.

Immobilized Al^{3+}–chelate chromatography and HPLC were also used to separate [α-^{32}P]N_3GTP-modified tryptic fragments. Photolabeled GDH was digested with trypsin and

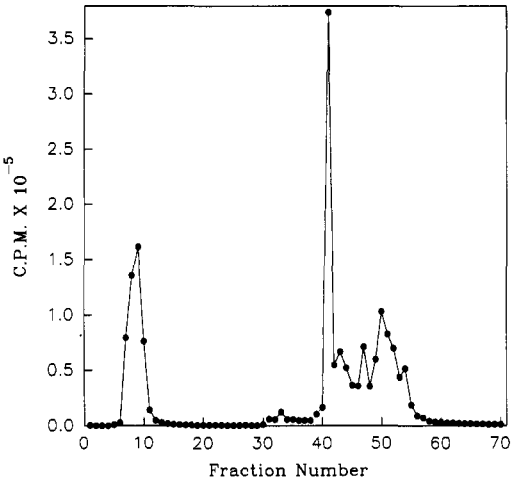

FIGURE 6: Radioactivity profile of HPLC of fractions eluted from Fe^{3+}–chelate chromatography. GDH was photolabeled with [α-^{32}P]$8N_3$GTP and digested with trypsin. Fractions from K_2HPO_4 elution from Fe^{3+}–chelate chromatography were loaded onto HPLC as described in Materials and Methods. One-minute fractions were collected, and ^{32}P incorporation was determined by scintillation.

subjected to Al^{3+}–chelate chromatography. The radioactive profile was similar to that of the chymotryptic procedure (see Figure 4) with the exception that the retention times for the radiolabeled peptides were different. The radiolabeled P_i eluate was subjected to HPLC as done for the chymotryptic experiment. Four radioactive peaks were observed (data not shown). The first peak was associated with the flow-through and contained no peptide. Two major radioactive peaks (fraction 38 and fraction 40) were sequenced and found to represent peptides corresponding to residues 439–447 and 439–452, respectively. According to the UV and radioactive profile from HPLC, the picomolar amounts of the third peak (fraction 42) were much lower than those of the major peaks and no sequence was obtained. Again, 300 μM GTP was able to eliminate photoinsertion into this peptide if present during photolysis (data not shown).

The identification of the [α-^{32}P]$8N_3$GTP-modified peptide was further confirmed using a Fe^{3+}–chelate resin. GDH modified with [α-^{32}P]$8N_3$GTP was treated with trypsin overnight as described and treated with Fe^{3+}–chelate chromatography using the same washes as used with the Al^{3+}–chelate resin. Virtually no radioactivity was associated with the flow-through fractions or the subsequent wash fractions. When 5 mM K_2HPO_4 was applied to the column, the radioactivity was eluted in 2–3 fractions. This procedure was repeated several times with or without a prior SP 25 ion-exclusion chromatography step. This step was included prior to metal–chelate chromatography in order to separate acidic peptides from the remaining species in the digestion mix. It was found that SP 25 chromatography prior to Fe^{3+}–chelate chromatography did not affect the final yield of photolabeled peptide(s) or increase the purity of the P_i eluted peptides, so this step was omitted most of the time.

After elution from the Fe^{3+}–chelate resin, the radioactive samples were prepared for reversed-phase HPLC. This particular procedure was repeated several times, and in all experiments, the radioactivity on HPLC coeluted with fraction 41 or 42 corresponding to 51–53% buffer B (see Figure 6). This peak was identified as the tryptic peptide containing residues 439–458 (Table IV). In one case both tryptic peptides 135–146 and 439–458 were identified from sequencing. However, the fragment 135–146 was identified only once from Fe^{3+}–chelate and never from Al^{3+}–chelate chromatography,

Table IV: Sequence Analysis of the Photolabeled Tryptic Peptide from the Radioactive Peak at 41 min in the HPLC Radioactive Profile from Figure 6

cycle	identified residue	fraction number 41
1	I	161[a]
2	S	70
3	G	97
4	A	126
5	S	47
6	E	82
7	K	13
8	D	39
9	I	75
10	V	67
11	H	13
12	S	17
13	G	41
14	L	35
15	A	26

[a] Picomoles.

while peptide 439–458 was consistently identified in all experiments. It is possible that the sequence 135–146 was retained on the Fe^{3+}–chelate resin due to the presence of four acidic residues in a span of five residues within the sequence (Asp138-Glu-Asp-Leu-Glu142). As in the case of the aluminum–chelate resin, GTP, present during photolysis, was able to protect the peptide from photomodification, and this peptide was not retained on the Fe^{3+}–chelate affinity resin.

DISCUSSION

Bovine glutamate dehydrogenase, a complex multimeric enzyme which integrates amino acid metabolism, is regulated by several nucleotide factors including NADH, ADP, and GTP. In a previous report from this laboratory, the adenine domain of the NAD^+ binding site was identified as Gly274-Glu275 (Kim & Haley, 1991). In the present report, it is shown that GDH is reversibly inhibited by $8N_3$GTP and can be photolabeled with the nucleotide analogs [α-^{32}P]$8N_3$GTP or [γ-^{32}P]$8N_3$GTP. Under the experimental conditions described, the photoinsertion into GDH was saturated with about 25–30 μM [γ-^{32}P]$8N_3$GTP. The apparent K_d of this interaction was 9 μM (Figure 2). The prevention of photoinsertion of [^{32}P]$8N_3$GTP (40 μM) by GTP (half maximal at 12 μM) demonstrates that the photoprobe is inserting into a specific GTP site within GDH. Other purine nucleotides including GDP, ATP, ADP, and NADH could reduce photolabeling with this probe, but not as effectively as GTP. Since GDH is suggested to contain several distinct but overlapping nucleotide binding sites (Jacobson & Colman, 1983), adenine nucleotides would be expected to reduce the binding of GTP to GDH and seem to do so (Goldin & Frieden, 1971).

$8N_3$GTP mimicked GTP in inhibiting the activity of GDH. The K_i of $8N_3$GTP for the enzyme was approximately 5 μM while that for GTP was 0.6 μM. Others have reported similar K_i values for GTP although these values have varied somewhat (Frieden, 1963; McCarthy & Tipton, 1984). In a similar experiment, $8N_3$ADP was able to increase the activity of GDH as effectively as ADP (data not shown).

A common argument against the use of 8-azidopurine nucleotides is that at equilibrium they exist primarily in the syn conformation rather than the anti conformation that characterizes the natural nucleotides. However, the data presented here showing the effects of $8N_3$GTP on GDH activity, and the protection from photolabeling by GTP, suggest that this probe interacts in the GTP binding domain in a

conformation that is similar enough to that of GTP to be a good biomimic of GTP. Also, if the $8N_3GTP$ bound to the GTP site without having to orient the 2 and 6 positions of the guanine ring properly, then this site should also bind ATP since these nucleotides differ only in these positions. Nucleotide binding sites that retain the very specific requirement for the guanine or adenine ring, when binding one of the 8-azidopurine probes of GTP, ATP, etc., must bind that photoprobe with the base rotated close to that of the natural nucleotide. This allows proper hydrogen bonding between the base and the binding domain amino acid residues and these interactions are what define the selectivity of binding.

In an earlier report, it was suggested that there are two binding sites for GTP per subunit, one independent of NADH and the other NADH-dependent (Pal & Colman, 1979). However, we have detected only one GTP binding site which is NADH-independent. NADH and NADPH are able to decrease photolabeling of GDH with $[^{32}P]8N_3GTP$ even at supersaturating concentrations (60 μM). Also, $[^{32}P]8N_3GTP$ saturation studies in the presence of NADH failed to reveal a second GTP binding site over a range of 0.1–250 μM photoprobe. It is unclear how NADPH or NADH affect the GDH–GTP interaction. It is possible that NADH induces a conformational change whereby GTP has an altered affinity toward the enzyme or is bound in a position that results in less efficient photoinsertion. NADH reportedly decreases the K_i of GTP for the enzyme (Frieden, 1963). In that study, NADH and GTP may have reduced the polymerization state of the enzyme (Fisher et al., 1972). However, in our studies the concentration of GDH is well below the critical concentration for aggregation (Cohen et al., 1976; Tipton & Couee, 1988). Our results do not indicate that there are two GTP binding sites within each GDH subunit.

The GTP–Mg^{2+} complex has been reported to have no effect on the enzyme while GTP at the same concentration will inhibit enzymatic activity (McCarthy & Tipton, 1984). In our study, the divalent cations, Mg^{2+} and Ca^{2+} (10 mM), were able to inhibit photolabeling 70%. Since $8N_3GTP$ and GTP bind Mg^{2+} tightly under these conditions, the ineffectiveness of the Mg^{2+}–GTP complex to inhibit activity can be explained by the decreased affinity of the enzyme toward the metal–nucleotide complex.

The photoinsertion site of $8N_3GTP$ into GDH has been identified as the peptide containing residues from Ile439 to Tyr454. This was verified using two different proteases and two different isolation procedures. Due to the lability of the *N*-glycosyl bond during HPLC (King et al., 1991) and the nonselectivity of the nitrene for any particular residues, it is difficult to determine the exact amino acid at the site of photoinsertion. The amount of Lys445 identified is less than that of the surrounding residues, and trypsin seems unable to cleave at this residue. Therefore, it may be a good candidate as the site of photoinsertion with $8N_3GTP$. However, while the peptide domain can be identified with confidence, the modified residue(s) cannot be unequivocally identified. This peptide could be 95% protected from photolabeling by the presence of 300 μM GTP demonstrating selectivity of the probe for the GTP binding site.

In another study using the classical chemical probe 5′-*p*-(fluorosulfonyl)benzoyl-1,N^6-ethenoadenosine (5′FSBεA), the guanine binding region was reported to contain the tryptic peptide Tyr262–Arg265 with Tyr262 being the residue identified as specifically interacting with the purine ring (Jacobson & Colman, 1984). It is unclear why 5′FSBεA, a hydrophobic adenosine-containing probe, should preferentially bind and react at a hydrophilic GTP binding site and not react at the other adenosine binding sites, especially with the absence of any distinguishing features which would render it a specific GTP probe. Perhaps the need to solubilize 5′FSBεA in dimethylformamide before addition could affect the protein–nucleotide interactions. Our results, though, show that $8N_3$-GTP specifically reacts at the guanine binding domain. In an earlier study, it was shown that the analogs $8N_3GTP$ and $8N_3GTP$ are able to recognize the respective ATP and GTP binding sites specifically and exclusively on eukaryotic polypeptide chain initiation factor 2 (Dholakia et al., 1989). In the present study, GTP, but not ATP, was able to compete for binding with a low micromolar K_d even with high concentrations of photoprobe (40 μM), and $8N_3GTP$ was able to inhibit GDH activity nearly as well as GTP.

Although a crystal formation suitable for X-ray analysis of bovine liver GDH has been difficult to obtain, the structure of GDH from other sources has been characterized. The subunits from *Clostridium symbiosum* were found to consist of two globular domains separated by a deep cleft (Rice et al., 1987; Stillman et al., 1992). This coenzyme binding region is speculated to be deep within this cleft which is consistent with peptide obtained in our laboratory that we have identified as modified with the photoprobe $[\alpha\text{-}^{32}P]2N_3NAD^+$. A three-dimensional analysis of mammalian liver enzyme is unavailable; however, the regulatory purine nucleotide binding sites are thought to reside in the C-terminal half of GDH (Smith et al., 1977).

GDH from *Neurospora crassa* is not regulated by ADP or GTP. This enzyme contains 48 less residues than bovine liver GDH, and there is little homology between the 100 residues in the C-terminus (Wootton et al., 1974). Studies have shown that chemical probes can at least partially desensitize bovine GDH to GTP inhibition while not affecting catalytic activity. The amino acids modified by these chemical probes were shown to reside in the C-terminus (Coffee et al., 1971; Piszkiewicz et al., 1971). It then seems likely that the regulatory ADP and GTP binding domains are located in this region. An analysis of the three-dimensional structure of the mammalian enzyme should supplement the understanding of the nature and location of these regulatory sites.

The methods of purification of the photolabeled peptides involve the use of aluminum(III)– and iron(III)–chelate affinity chromatography. Metal–chelate affinity chromatography has been used to separate phosphorylated amino acids and peptides from nonphosphorylated ones due to their ability to retain phosphorylated species with a good degree of selectivity through nonionic coordination chemistry (Anderson, 1991; Scanff et al., 1991). The use of these metal–chelate affinity chromatographic methods is an advancement in the purification of azidonucleotide-photomodified peptides as well. This laboratory has used Fe^{3+}–chelate affinity chromatography successfully to identify the nucleotide binding peptides from adenylate kinase, botulinum toxin C3 enzyme, and rhGM-CSF (Salvucci et al., 1992; Chavan et al., 1992; Doukas et al., 1992).

The photolabeled peptides from GDH were purified and identified by either Al^{3+} or Fe^{3+}–chelate chromatography from tryptic and chymotryptic digests. Both methods were able to successfully retain the radiolabel of photolabeled peptides. We have observed that they have very high affinity for the triphosphate of the photoinserted probe and may be used in a single step to isolate only photolabeled peptides from a very complex peptide mixture. Also, with this technique excess protease may be added without a problem since we have never

observed any peptide fragments of the proteases being retained. Once photolabeled peptides are bound to the metal–chelate resin, they can be washed with 100 mM ammonium acetate solutions containing 0.5 M NaCl or 4 M urea to elute any peptides that may be bound to the resin other than through phosphate–metal interactions. The specificity of the Al^{3+} resin has been demonstrated by its ability to retain only the photomodified (N-terminal) peptide from glucagon while the other peptides were associated with the flow-through including the same (N-terminal) peptide when left unmodified (unpublished data). In the case of GDH, Figure 5 demonstrates the specificity of this resin. The flow-through fractions from Al^{3+}–chelate affinity chromatography had a multitude of peptides associated with then, while the phosphate eluate contained only three UV peaks from HPLC, one of which was radioactive. When these columns are used, caution should by used when interpreting the UV absorbance profile. In blank runs without peptides, certain spurious UV absorbing peaks were detected due to chromophore elution from the metal–chelate columns. This is especially a problem when low quantities of peptide are being isolated.

The use of metal–chelate enhances the recovery of photolabeled peptides because it reduces the number of separation steps to just two. The amount of recovered peptides was about the same regardless of which metal–chelate resin was used prior to HPLC. Although both metal–chelate resins are able to successfully retain the photolabeled peptides, the Al^{3+}–chelate resin has an advantage in that it is more selective toward the photolabeled peptides. In two other studies, the Fe^{3+}–chelate resin retained other peptides which are rich in acidic residues, whereas the Al^{3+}–chelate resin retained only azidonucleotide-modified peptides with very little contaminants possibly due to the Al^{3+}–chelate resin's greater selectivity for phosphate versus carboxylate groups. In studies involving tubulin, creatine kinase, and GDH, our laboratory has found that the Al^{3+}–chelate resin does not retain the nonphotolabeled, carboxylate-rich peptides as does the Fe^{3+}–chelate resin. This was especially true of tubulin where the carboxylic-rich C-terminal was always present in the Fe^{3+}–chelate resin isolations but not when the Al^{3+} resin was used (Jayaram and Haley).[2] These results indicate that Al^{3+}–chelate chromatography could prove to be a more effective general way of isolating azidonucleotide-photomodified peptides than the Fe^{3+} resin procedure.

REFERENCES

Anderson, L. (1991) *J. Chromatogr. 539*, 327–334.

Bitensky, M., Yielding, K., & Tomkins, G. (1965) *J. Biol. Chem. 240*, 1077–1082.

Chavan, A., Nemoto, Y., Narumiya, S., Kozak, S., & Haley, B. (1992) *J. Biol. Chem. 267*, 14866–14870.

Coffee, C., Bradshaw, R., Goldin, B., & Frieden, C. (1971) *Biochemistry 10*, 3516–3526.

Cohen, R., Jedziniak, J., & Benedek, G. (1976) *J. Mol. Biol. 108*, 179–199.

Dholakia, J., Francis, B., Haley, B., & Wahba, A. (1989) *J. Biol. Chem. 264*, 20638–20642.

Doukas, M., Chavan, A., Gass, C., Boone, T., & Haley, B. (1992) *Bioconjug. Chem. 3*, 484–492.

Erecinska, M., & Nelson, D. (1990) *J. Neurochem. 54*, 1335–1343.

Fahien, L., Teller, J., MacDonald, M., & Fahien, C. (1990) *Mol. Pharmacol. 37*, 943–949.

Fisher, H., Culver, J., & Prough, R. (1972) *Biochem. Biophys. Res. Commun. 46*, 1462–1468.

Fonnum, F. (1984) *J. Neurochem. 42*, 1–10.

Frieden, C. (1963) *J. Biol. Chem. 238*, 3286–3300.

Geahlen, R., & Haley, B. (1977) *Proc. Natl. Acad. Sci. U.S.A. 74*, 4375–4377.

Geahlen, R., & Haley, B. (1979) *J. Biol. Chem. 254*, 11982–11987.

Goldin, B., & Frieden, C. (1971) *Curr. Top. Cell. Regul. 4*, 77–117.

Hoyer, P., Fletcher, P., & Haley, B. (1986) *Arch. Biochem. Biophys. 245*, 369–378.

Jacobson, M., & Colman, R. (1983) *Biochemistry 22*, 4247–4257.

Jacobson, M., & Colman, R. (1984) *Biochemistry 23*, 6377–6382.

Kim, H., & Haley, B. (1991) *Bioconjug. Chem. 2*, 142–147.

King, S., Kim, H., & Haley, B. (1991) *Methods Enzymol. 196*, 449–466.

McCarthy, A., & Tipton, K. (1984) *Biochem. J. 220*, 853–855.

Moon, K., Piszkiewicz, D., & Smith, E. (1972) *Proc. Natl. Acad. Sci. U.S.A. 69*, 1380–1383.

Pal, P., & Colman, R. (1979) *Biochemistry 18*, 838–845.

Piszkiewicz, B., Landon, M., & Smith, E. (1971) *J. Biol. Chem. 246*, 1324–1329.

Plaitakis, A., & Berl, S. (1988) in *Glutamine and Glutamate in Mammals* (Kvamme, E., Ed.) Vol. II, pp 127–142, CRC Press, Inc., Boca Raton, FL.

Potter, R., & Haley, B. (1983) *Methods Enzymol. 91*, 613–633.

Rice, D., Baker, P., Farrants, G., & Hornby, D. (1987) *Biochem. J. 242*, 789–95.

Salvucci, M., Chavan, A., & Haley, B., (1992) *Biochemistry 31*, 4479–4487.

Scanff, P., Yvon, M., & Pelissier, J. (1991) *J. Chromatogr. 539*, 425–432.

Shoemaker, M., Lin, P., & Haley, B. (1992) *Protein Sci. 1*, 884–891.

Smith, E., Austen, B., Blumenthal, K., & Nyc, J. (1975) in *The Enzymes* (Boyer, P., Ed.) Vol. 11, pp 293–367, Academic Press, New York.

Stillman, T., Baker, P., Britton, K., Rice, D., & Rodgers, H. (1992) *J. Mol. Biol. 224*, 1181–1184.

Tipton, K., & Couee, I. (1988) in *Glutamine and Glutamate in Mammals* (Kvamme, E., Ed.) Vol. I, pp 81–100, CRC Press, Inc., Boca Raton, FL.

Tomkins, G., Yielding, K., Talal, N., & Curran, J. (1963) *Cold Spring Harbor Symp. Quant. Biol. 28*, 461–471.

Wootton, J., Chambers, G., holder, A., Baron, A., Taylor, J., Fincham, J., Blumenthal, K., Moon, K., & Smith, E. (1974) *Proc. Natl. Acad. Sci. U.S.A. 71*, 4361–4365.